An empirical model for interferometric coherence

Chaabane F. [a], Tupin F. [b] and Maître H. [b]

[a] URISA-SUP'COM, 3.5 route de Raoued, 2083 Ariana, Tunisie
[b] GET-Télécom-Paris - CNRS URA 820, 46 rue Barrault, 75013 Paris, France

ABSTRACT

Many are the examples of application of SAR and differential SAR interferometry for topographic mapping and ground deformation monitoring. However, on repeat pass geometry, the performance of these two techniques is limited by the problem of loss of correlation (coherence) between two radar acquisitions. The lack of coherence causes an additional noise thus a bad estimate of the interferometric phase. The disturbances can be due either to surface changes due to long period cover (temporal decorrelation) or to a strong value of the baseline (spatial decorrelation).

In this paper, we propose an empirical model for the estimate of coherence considering separately these two sources of disturbances. Starting from the observations of experimental data, we study the behaviour of coherence according to baseline and period cover in order to express the two terms of correlation. A number of 170 multi temporal and multi baseline differential interferograms covering the same region is used to validate the proposed model.

Keywords: SAR interferometry, interferometric phase, coherence, temporal and spatial decorrelation

1. INTRODUCTION

SAR and differential SAR interferometry[1] have proven to be a performant tools for measuring with great accuracy topography profile and ground surface motion.[2–4] However, accurate estimation of the correlation or coherence between channels is necessary. It is applied to select areas in which the phase information can be used to extract target height as well as an indication of the quality of the generated digital elevation model.[5] In an other hand, a perfect knowloge of the coherence is crucial for ground moving target measurements.[6] Thus, quantitave coherence information is very important and should be estimated accurately.[7]

The SAR phase difference is a relevant information only if it is calculated between two images acquired in the same conditions especially in repeat passes over the same site. This constraint represent an important limitation of SAR interferometry. The phase can be disturbed by various types of phenomena. One of the principal disturbances is the loss of correlation between two acquisitions which induces a bad estimation of the phase thus a bad estimation of topography by interferometry. There is essentially two kind of disturbances causing decorrelation[1,8]:

- temporal decorrelation : ground surface changes due to long period cover such us vegetation grouth, glacier motion, soil moisture, etc.
- spatial decorrelation : sensor geometry changes between the two radar acquisition. It concerne the repeat incidence and aspect angles. This effect is directly related to the distance between the two antennas i.e. the baseline.

This paper presents the different sources contributing to decorrelation, discuss correlation factors estimation existing in the litterature and give a new empirical model for coherence by considering separetely the two latter effects.

The second section present some theoretical bases useful in determining interferometric phase and coherence statistical models. Both single and multi-look processing are considered. In section three, we describe the various sources of decorrelation. The different factors causing a loss of correlation are considered separetely. The total correlation is then given by the product of the different contribution factors. The section four propose a new empirical model for interferometric coherence which is validated on experimental data. The proposed model isolate spatial and temporal decorrelation. Spatial decorrelation formulation is confirmed with what exist in the litterature but new temporal decorrelation formulation is much easier to determine when knowing surface ground features.

2. INTERFEROMETRY BASES

Single-look complex radar signal is the starting point of interferometric statistical models study. Most mathematical modeling is aiming at the single-look processed data. However, for speckle reduction and data compression, interferometric radar data are frequently multi-look processed.

Considering the circular Gaussian assumption[9] applied to two different radar signals z_1 and z_2, we deduce the joint probability density function which is also a circular Gaussian distribution:

$$pdf(z_1, z_2) = pdf(Z) = \frac{1}{\pi^2 det(C_Z)} exp(Z^{-t*} C_Z^{-1} Z). \tag{1}$$

where Z is the complex vector (z_1, z_2), Z^{-t*} the complex conjugate transpose of Z and C_Z is the complex covariance matrix of Z given by:

$$C_z = \begin{pmatrix} E[|z_1|^2] & E[z_1^* z_2] \\ E[z_1^* z_2] & E[|z_2|^2] \end{pmatrix} \tag{2}$$

The diagonal elements of this matrix corresponds to averaged intensities whereas the nondiagonal elements provide the complex correlation between the two images.

$$\gamma = \rho e^{j\phi_0} = \frac{E[z_1^* z_2]}{\sqrt{E[|z_1|^2] E[|z_2|^2]}} \tag{3}$$

with $\rho = |\gamma|$, denotes the coherence or the correlation coefficient between the two Gaussian signals and $\phi_0 = arg(\gamma)$ is the phase difference between z_1 and z_2 thus the required interferometric phase.

The statistics presented above are calculated only for one resolution element (Single-look) in one interferogram. However, the interferometric coherence and phase are frequently calculated on several samples (multi-look). Multiple neighboring pixels are averaged in order to reduce the speckle in the inteferogram. For L looks, the experimental complex covariance matrix is given by:

$$C = \frac{1}{L} \sum_{k=1}^{L} Z_k Z_k^{t*} \tag{4}$$

The diagonal elements of this matrix provide an experimental phase $\hat{\phi}$ and an experimental correlation $\hat{\rho}$ used as interferometric data. The expression of $\hat{\phi}$ and $\hat{\rho}$ is written:

$$\begin{cases} \hat{\phi} = arg(\gamma) \\ \hat{\rho} = |\gamma| \end{cases} \tag{5}$$

$$with \qquad \gamma = \frac{\sum_{k=1}^{L} z_{1,k} z_{2,k}^*}{\sqrt{\sum_{k=1}^{L} z_{1,k} z_{1,k}^*} \sqrt{\sum_{k=1}^{L} z_{2,k} z_{2,k}^*}} \tag{6}$$

The two estimators $\hat{\phi}$ and $\hat{\rho}$ are also ML (Maximum Likelihood) estimators.[7] It should be noted that the multi-looking processing will not improve the coherence but will reduce the standard deviation of the interferometric phase.

3. STATISTICAL LIMITATION : DECORRELATION

The interferometric coherence given by the equation 5, identify the regions where variations of the phase between two acquisitions are correlated. The experimental coherence $\hat{\rho}$ measures the degree of similarity between two radar images since it represent a statistical estimator of the complex correlation coefficient. The coherence highlights thus the quality and the potential of an interferometric couple.

Since interferometric measurements are disturbed by various phenomena, a loss of coherence between the two radar images appears. It induces a visible noise in the interferogram affecting any estimate of the phase and values of $|\gamma|$ close to zero. There is several causes to explain the problem of decorrelation[10]:

1. The retrodiffused signals are disturbed with an additive thermal noise related to the sensor.
2. Effects due to interferometric radar geometry. There is essentially three sources of geometrical decorrelation:
   - The changes caused by viewing the surface with two antennas at slightly different aspect angles. That induces a change of the relative positions of the diffusers within the pixel. The degree of coherence will be then a function of the distance separating the two satellite positions i.e. the interferometric baseline.
   - The changes caused by pixel misregistration between the two InSAR images. The scattering targets for the two pixels are slightly different and therefore have different interference patterns.
   - The third geometrical effect inducing a decorrelation is the rotation of the targets with respect to the radar look direction. The rotation of a resolution element yields to slightly different phase shift resulting in signal decorrelation.
3. Two radar acquisitions are separate in time (case of multi-pass) so there is a temporal decorrelation. This term is caused by changes of the physical surface features, phenomenon difficult to predict or to model. Modifications of the distribution of the resolution element can be du to different causes involving the displacement of the sources (growth of the vegetation, rivers...) and/or a modification of the electromagnetic features of the targets (moisture, temperature ...).

According to what precedes, Zebker et al..[8] showed that the total term of decorrelation is written:

$$\hat{\rho}_{total} = \hat{\rho}_{thermal} \cdot \hat{\rho}_{geometrical} \cdot \hat{\rho}_{temporal} \tag{7}$$

Li and Goldstein[11] like Rodriguez and Martin[12] quantified these various contributions to the decorrelation using one statistical model of formation of the images starting from elementary targets. This work was then resumed and improved by Zebker in.[8]

3.1. Thermal decorrelation

The loss of correlation related to thermal noise is obtained by considering two signals acquired by two different antennas, observing the same target, at the same moment. These signals are then modelled by the sum of a commun correlated part and an additional thermal noise. The thermal decorrelation is given by:

$$\hat{\rho}_{thermal} = \frac{1}{1 + RSB^{-1}} \tag{8}$$

where RSB the signal to noise ratio.

3.1.1. Geometrical decorrelation

The spatial decorrelation caused by three different sources, we start by presenting the baseline decorrelation. It is obtained by adding the uncorrelated part of the signal to preceding modeling of the two received signals. It's given by:

$$\hat{\rho}_{baseline} = 1 - \frac{2BRes_x}{\lambda R_0} \tag{9}$$

where B is the baseline, Res_x and R_0 are the range resolution and the target satellite distance. the correlation decrease quickly when B increase. The minimum value of B for which $\hat{\rho}_{baseline}$ equals zero is the critical baseline B_c:

$$B_{c\perp} = \frac{\lambda R_0 \cos\theta}{2Res_x}$$

This equation underlines the importance of the baseline for an interferometric couple. For differential interferometry dedicated to surface change measurements, similar radar geometries are desirable, i.e. the lowest value of the baseline. However, for interferometry dedicated to topography mapping, significant values of baseline are desirable because it increases the altitude sensitivity. Then, it is obvious that the baseline controls the quality of an interferogram and it should not exceed the critical baseline.

An error of pixel misregistration introduces a phase shift which involves a loss of correlation given by:

$$\hat{\rho}_{misregsitration} = sinc(\frac{\pi\Delta x}{Res_x}(1 - \frac{2BRes_x}{\lambda R_0}))$$

where Δx represent an error of misregistration on the ground. Only significant errors of misregistration approaching the size of the pixel will involve a significant loss of correlation.

Finally, a rotation angle $d\phi$ of the targets with respect to the look direction induce a decorrelation given by:

$$\hat{\rho}_{rotation} = 1\frac{2\sin\theta|d\phi|Res_y}{\lambda}$$

where Res_y is the azimuth resolution.

3.1.2. Temporal decorrelation

A quantification of the temporal correlation due to the change of surface was given by Zebker and Al in.[5] It measure the volumic change of a resolution element by considering the influence of a random horizontal change σ_x, and a random change in height σ_z. The temporal decorrelation is then given by:

$$\hat{\rho}_{temporal} = \exp\{-\frac{1}{2}(\frac{4\pi}{\lambda})^2(\sigma_x^2 \sin^2\theta + \sigma_z^2 \cos^2\theta)\} \tag{10}$$

Only random motions are considered, that is, each scattering center moves independently from all others.If in fact the scatterers move together in one prefered direction then instead of decorrelation a systematic phase shift would occur.

In conclusion, for differential interferometry, it is preferable to use on one hand, interferograms with small baseline to reduce spatial decorrelation, and in other hand, to use short period couples to limit temporal decorrelation.

To resolve decorrelation problems (thermal, geometric of temporal) affecting the interferometric phase, several solutions were proposed in particular the interferogram filtering[13].[14]

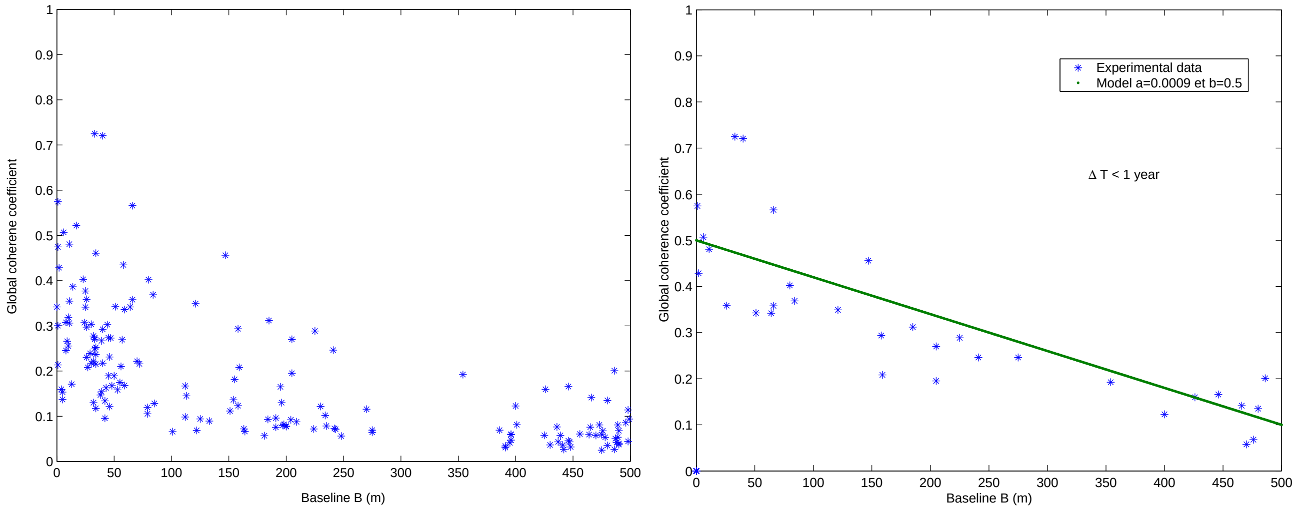

Figure 1. Global coherence coefficient variation according to baseline for a data set of 170 interferograms. Interferograms time period is thresholded to one year (right figure) to reduce temporal decorrelation effects.

4. EMPIRICAL MODEL FOR COHERENCE

The coherence is a measurement of the interferometric phase standard deviation and depends primarily on satellite parameters, imaging geometry and ground features. The equation 7 shows that coherence is written as a product of three quantities. Usually, the geometrical and temporal correlation are more significant than thermal correlation. Thus, we can make the assumption that the noise of the sensor is negligible, so that coherence will incorporate only two quantities : geometrical and temporal correlation.

$$\hat{\rho}_{total} \simeq \hat{\rho}_{geometrical} \cdot \hat{\rho}_{temporal} \tag{11}$$

Having a multi-temporal and multi-baseline series of 170 differential interferograms covering the region of Corinth Gulf, we study the behavior of coherence according to baseline and time period in order to express the two terms of correlation $\hat{\rho}_{geometric}$ and $\hat{\rho}_{temporal}$. It follows an empirical modeling of these two quantities.

For this purpose, we attribute to each interferogram a global coherence coefficient reflecting its quality. Global coherence coefficient is calculated using the coherence image provided by Diapason [] which is calculated starting from the equations 5 and 6.

4.1. Geometrical decorrelation

As previously mentionned, the geometrical correlation is due to three different causes. Assuming that the two satellite orbits are parallels and the misregistration errors are less than pixel size, the geometrical decorrelation is then attributed to the change of satellite position between the two acquisitions.

Variations of the global coherence coefficient with respect to baseline are plotted in figure 1. However, this coefficient incorporate the baseline and time decorrelation effects mixed together. In order to reduce temporal effects, we threshold the baseline to $100m$, obtaining thus figure 1. This figure, shows in accordance with equation 9, that we can make the assumption of a linear relation ship between the correlation and baseline which can be written by

$$\hat{\rho}_{geometrique} = aB + b \tag{12}$$

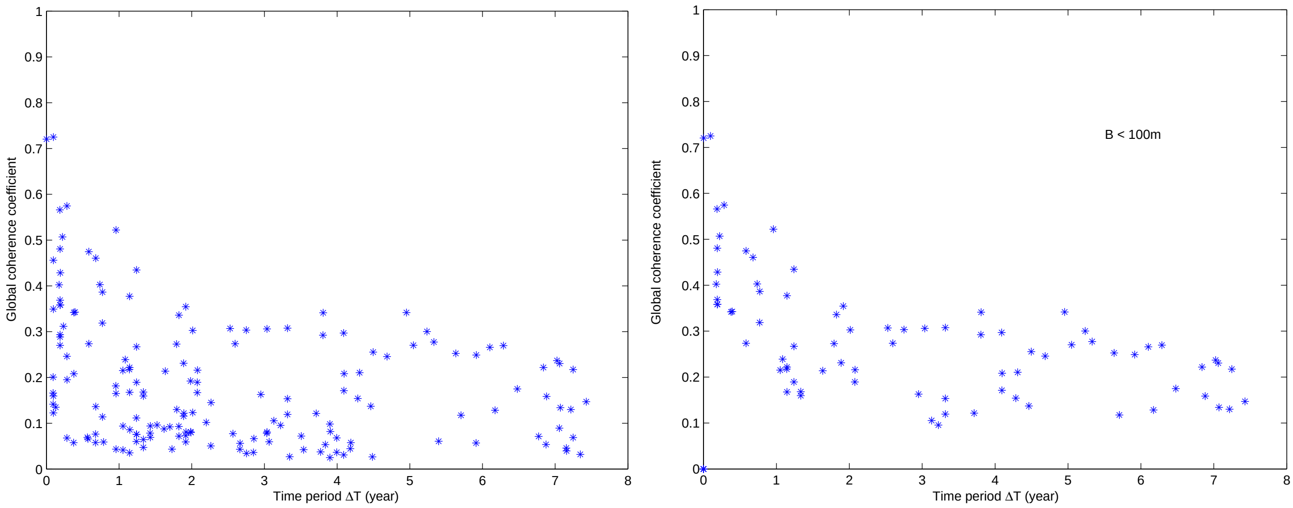

Figure 2. Global coherence coefficient variation according to time period for a data set of 170 interferograms. Interferograms baseline is thresholded to $100m$ (right figure) to reduce geometrical decorrelation effects.

Knowing that maximum correlation ($\hat{\rho}_{geometrical} = 1$) is realized for a zero baseline. We deduce that $b = 1$. This value does not correspond to the experimental value of b since we cannot completely isolate baseline effect from temporal one. The value of the experimental slope a obtained is:

$$ac = -0.001 \simeq -\frac{1}{Bc_{ERS}} \tag{13}$$

where Bc_{ERS} is the critical baseline of satellite ERS estimated at $1100m$. The expression of the equation 9 established by Zebker[8] is thus confirmed with experimental results.

Consequently, the geometrical correlation can be modelled by:

$$\hat{\rho}_{geometrique} = 1 - \frac{B}{Bc} \tag{14}$$

4.1.1. Temporal decorrelation

Variations of the global coherence coefficient with respect to period of time covered by the interferogram are also plotted. In order to reduce baseline effect, we threshold time period to one year (see figure 2).

The figure 2 shows that the temporal correlation decrease exponentially according to time period. More the interferogram duration increase more the correlation has a significant decreases. However, temporal correlation is function of ground features in particular of surface ground changes. Therefore the figure 2 is not sufficient to determine temporal decorrelation, the global coherence coefficient is still biaised by the change of the ground nature. Assuming that the regions having the same ground surface properties undergoe the same changes (displacement or electromagnetic features change), the temporal correlation can be written:

$$\hat{\rho}_{temporelle} = exp(-\beta \Delta T^2) \tag{15}$$

where ΔT represent the interferogram period of time and β is a parameter related to the ground feature. Thus, having a classification of the ground surface components, we can estimate the value of the temporal correlation.

For the Corinth Gulf interferogram data base, a classification algorithm is applied on a landsat image (covering the same region than interferograms) in order to specify the areas of different cover. The classification algorithm used is the K-means. It enable us to determine three different classes of ground components (see figure 3). The value of β is then calculated by minimizing the difference between the model and the experimental data.

For two regions characterized by two different parameters β i.e. having different surface cover, the global coherence coefficient is plotted according to interferogram duration (see figure 4). The obtained figure shows that the model fit well data but as we can notice the exponential decrease is slithtly faster than the data one. This is du to the fact that the baseline is not the same for all interferograms (even thresholded). We can also see that the global coherence coefficient in the figure 4 (right one) is more significant than the one of figure 4 (left one). It's because rocky areas are more coherent than vegetation ones. The model suggested will not be valid in particular cases where the changes of ground surface touch only a delimited part of a region as for example vegetations areas half irrigated, areas deforested in parts, etc.

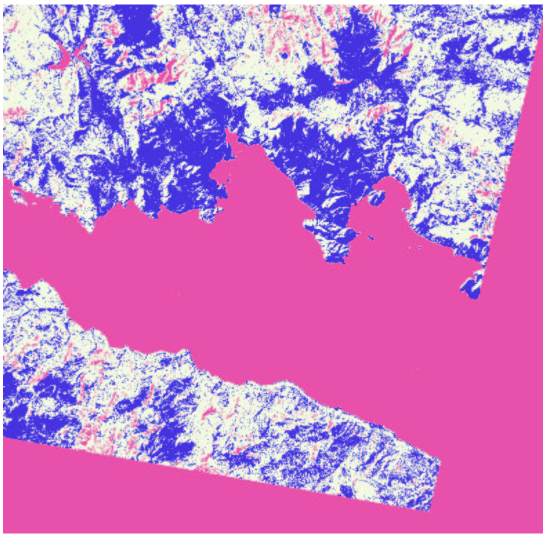

Figure 3. Landsat classification applied in order to fix ground areas with the same features. 3 classes are obtained corresponding respectively to vegetations (white), rocky areas (black) and water sufaces (gray).

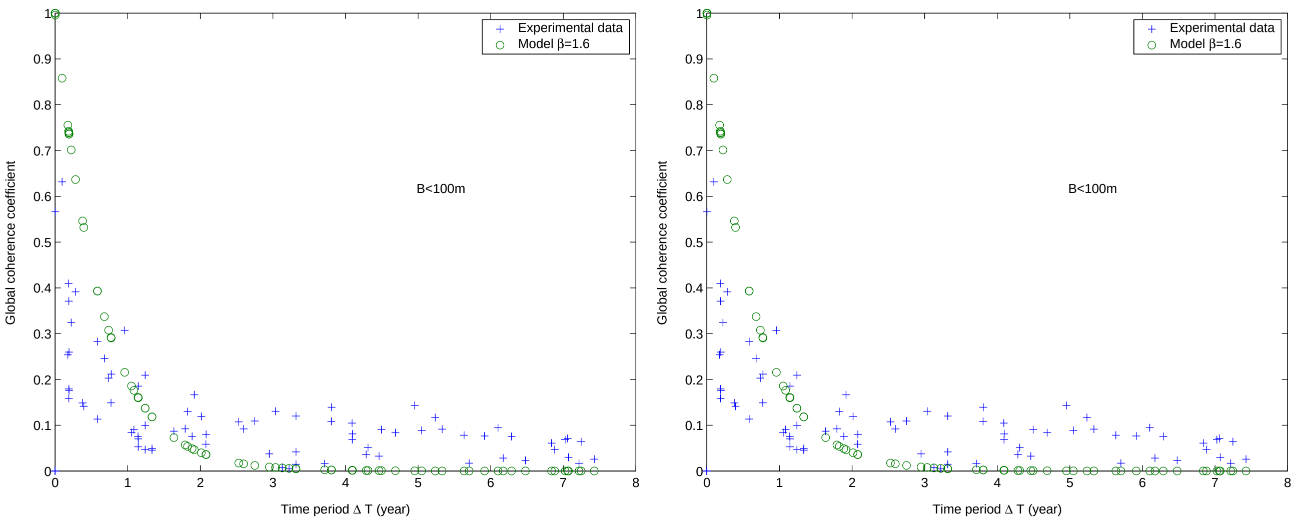

Figure 4. Temporal decorrelation models for two different ground surface cover regions. (left figure) temporal decorrelation for vegetation areas. (right figure) temporal decorrelation for rocky areas.

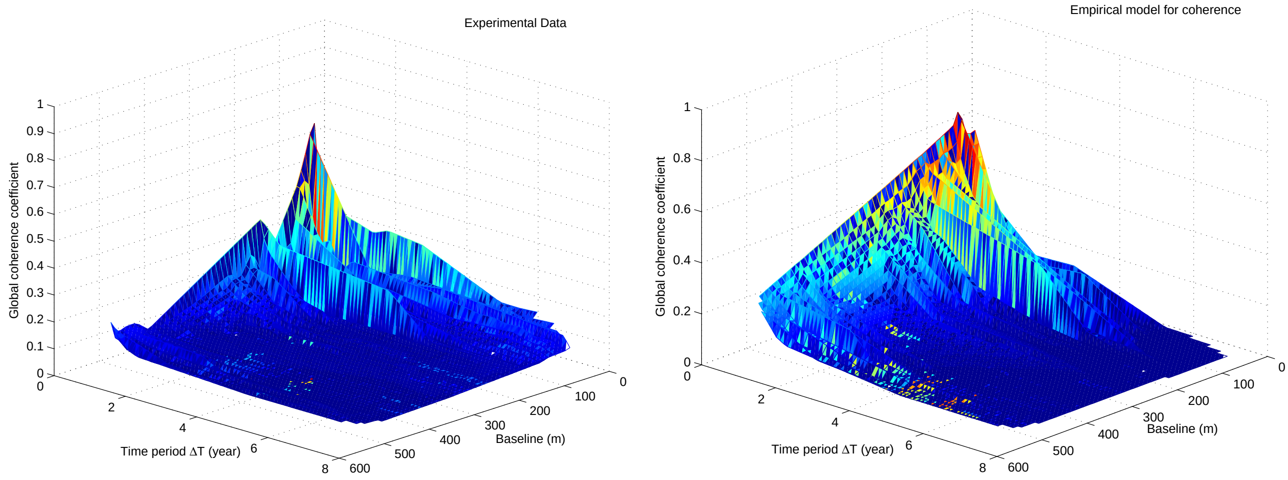

Figure 5. 3D variation of the global coherence coefficient according to baseline and time period for the data base of 170 differential interferograms. The right figure corresponds to the obtained empirical model for the same set of interferograms.

If we compare the expression of temporal correlation given by Zebker,[8] to the expression given by the equation 15, we notice two exponential decreases: one according to interferogram time period, the other according to scattering volume. The first formulation is more rigorous and is obtained with less approximations. However, in a practical way, it is very difficult, sometime impossible to measure the volume variation of each pixel which make the second expression easier to exploit.

Thus the total expression of the new coherence empirical estimator is given by:

$$\hat{\rho}_{total} = \hat{\rho}_{geometrique}\hat{\rho}_{temporelle} = (1\frac{B}{Bc})(exp(-\beta\Delta T^2)) \tag{16}$$

The figure 5 enables us to compare the variation of global coherence coefficient simultanously according to baseline and time period .It is obtained starting from the experimental data and from the empirical model. The two curves are close except for points where baseline decorrelation is biaised by temporal factor and inversely.

5. CONCLUSION

In this article, we exposed the problem of coherence estimation for SAR interferometric processing. An empirical model for interferometric coherence is proposed and was validated on a data set of 170 multi temporal and multi baseline interferograms. This model was also discussed and compared to other existant modeling and we showed that proposed formulation of temporal decorrelation is very useful in a practical way.

ACKNOWLEDGMENTS

The authors would like to thank Dr. P. Briole (Institut du Physique du Globe de Paris-IPGP) for providing the data base of multi temporal and multi baseline interferograms and for interesting discussions.

REFERENCES

1. P-A. Rosen, S. Hensley, I-R. Joughin, F-K. LI, S-N. Madsen, E. Rodriguez and R-M. Goldstein,"Synthetic Aperture Radar Interferometry," *Proceeding of IEEE.*, **3(88)**, pp. 333-382, march 2000.
2. A. Ferretti, C. Prati, and F. Rocca, "Permanent Scatterers in SAR Interferometry," *IEEE Trans. on Geoscience and Remote Sensing*, **1(39)**, pp. 8-20, January 2001.

3. F. Chaabane, F. Tupin and H. Matre "Combination of multiple interferograms for monitoring temporal evolution of ground deformation," *IEEE International Geoscience and Remote Sensing Symposium, IGARSS'04*, Alaska, September 2004.
4. G. Luzi, M. Pieraccini, D. Mecatti, L. Noferini, G. Guidi, F. Moia, and C. Atzeni, "Ground-Based Radar Interferometry for Landslides Monitoring: Atmospheric and Instrumental Decorrelation Sources on Experimental Data," *IEEE Trans. Geosci. and Remote Sensing* **11(42)**, pp. 2554-2466, November 2004.
5. H. A. Zebker and C. L. Werner and P. A. Rosen and S. Hensley, "Accuracy of Topographic Maps Derived from ERS-1 Interferometric Radar" *IEEE Trans. Geosci. and Remote Sensing*, **4(32)**, pp. 823-836, 1994.
6. C.H. Gierull, "Umbiaised coherence estimator for SAR interferometry with application to moving target detection," *ELECTRONICS LETTERS*, **14(37)**, pp. 913-915, July 2001.
7. R. Touzi and A. Lopes and J. Bruniquel and P. W. Vachon, "Coherence Estimation for SAR Imagery" *IEEE Trans. Geosci. and Remote Sensing*, **1(37)**, pp. 135-149, 1999.
8. H. A.Zebker and J. Villasenor, "Decorrelation in interferometric radar echoes," *IEEE Trans. Geosci. and Remote Sensing*, **5(30)**, pp. 950-959, 1992.
9. J. S. Lee and K. W. Hoppel and S. A. Mango and A. R. Miller, "Intensity and phase statistics of multilook polarimetric and interferometric SAR imagery" *IEEE Trans. Geosci. and Remote Sensing*, **5(32)**, pp. 1017-1028, 1994.
10. H. Maître (sous la direction de),"Le traitement des images de radar à synthèse d'ouverture" Hermès, Paris - Collection IC2,2001.
11. F.K. Li and R.M. Goldstein, "Studies of multibaseline spaceborne interferometric synthetic aperture radars," *IEEE Trans. Geosci. and Remote Sensing*, **1(28)**, pp. 88-97, 1990.
12. E. Rodriguez and J.M. Martin, "Theory and design of interferometric synthetic aperture radars" *IEE PROCEEDINGS-F*, **2(139)**,pp. 147-159, 1992.
13. E. Trouv, J.-M. Nicolas, and H. Maître, "Fringe detection in noisy complex interferograms," *Applied Optics - Information Processing*, **35**, pp. 3799-3806, 1996.
14. F. Chaabane, A. Avallone, F. Tupin, P. Briole and H. Maître, "Improvement of tropospheric correction by adapted phase filtering," *EUSAR2002*, Cologne, pp. 361-364, June 2002.